

The FLUKA nuclear cascade model applied to neutrino interactions

*NUINT'02 ,
December 12-15, 2002
University of California, Irvine*

G. Battistoni[†], A. Ferrari¹, A. Rubbia², P.R.Sala³

[†] INFN Milan

¹ CERN (on leave from INFN-Milan)

² ETH Zurich

³ ETH Zurich (on leave from INFN-Milan)

NUX-FLUKA

FLUKA

A. Fassò, A. Ferrari, J. Ranft,
P.R. Sala

Interaction and transport
MonteCarlo code

Hadronic and electromagnetic, from thermal neutrons to ≈ 100 TeV
see www.fluka.org

NUX

A. Rubbia

Neutrino-nucleon generator

Exclusive, all neutrino flavor, NC and CC, $10 \text{ MeV} < E_\nu < 10 \text{ TeV}$

See A. Rubbia talk at NUINT01

NUX-FLUKA

NUX events embedded in the FLUKA nuclear model
Event generation, Detector simulations (ICARUS)

ν in NUX-FLUKA

ν interactions Are performed like on free nucleon, but
Initial State effects (Fermi motion) and
Final State effects (Pauli, reinteractions,..)

Automatically taken into account by PEANUT, the low/intermediate energy hadron interaction model in FLUKA

PEANUT is a three step model:

(Generalized) IntraNuclear Cascade

+ Preequilibrium

+ Evaporation/Fission or Fermi break-up

I'll not describe here the high energy hadronic generator, that is based on the Dual Parton Model+Glauber cascade + GINC

(Generalized) IntraNuclear Cascade basic assumptions

1. Primary and secondary particles moving in the nuclear medium
2. Interaction probability (σ_{free} + Fermi) $\times \rho(r)$ + exceptions($\pi..$)
3. Classical trajectories (+) nuclear mean potential (resonant for π 's!!)
4. Curvature from nuclear potential \rightarrow refraction and reflection.
5. Interactions are incoherent and uncorrelated
6. Interactions in projectile-target nucleon CMS \rightarrow Lorentz boosts
7. Multibody absorption for π, μ^-, K^-
8. Quantum effects (Pauli, formation zone, correlations...)
9. Nuclear masses from tables or Cameron formula
10. Exact conservation of energy, momenta and all additive quantum numbers, including nuclear recoil

Preequilibrium

For $E > \pi$ production threshold \rightarrow only (G)INC models

At lower energies \rightarrow a variety of preequilibrium models

Two leading approaches

the quantum-mechanical multistep model

Very good theoretical background

complex, difficulties for multiple emission

the exciton model

statistical assumptions

simple and fast

Exciton model: chain of steps, each (n_{th}) step corresponding to N_n

“excitons” == either a particle above or a hole below the Fermi surface

Statistical assumption: any partition of the excitation energy E among N ,
 $N = N_h + N_p$, excitons has the same probability to occur

Step: nucleon-nucleon collision with $N_{n+1} = N_n + 2$ (“never come back” approximation)

Chain end = equilibrium = N_n sufficiently high or excitation energy below threshold

N_1 depends on the reaction type and on the cascade history

Preequilibrium : GDH

Preequilibrium emission probability:

$$P_{x,n}(\epsilon)d\epsilon = \sum n_{p_x} \frac{\rho_n(U, \epsilon)gd\epsilon}{\rho_n(E)} \frac{r_c(\epsilon)}{r_c(\epsilon) + r_+(\epsilon)}$$

where the density (MeV^{-1}) of exciton states is given by:

$$\rho_n(E) = \frac{g(gE)^{n-1}}{n!(n-1)!}$$

the emission rate in the continuum:

$$r_c = \sigma_{inv} \frac{\epsilon}{g_x} \frac{(2s+1) 8\pi m}{h^3}$$

and the reinteraction rate:

$$r_+(\epsilon) = f_{Pauli}(\epsilon, E_F) [\rho_p \sigma_{xp} + \rho_n \sigma_{xn}] \left[\frac{2(\epsilon + V)}{m} \right]^{1/2}$$

(or from optical potential)

GDH: ρ, E_F are “local” averages on the trajectory and constrained exciton state densities are used for the lowest lying exciton configurations.

Preequilibrium: modified GDH in PEANUT

- σ_{inv} from systematics
- Correlation/formation zone / hardcore effect on reinteractions:

$$\frac{r_c(\epsilon)}{r_c(\epsilon) + r_+(\epsilon)} \rightarrow P_c^{(h\tau)} + P_c^{(co)} + P_c^{(std)}$$

$P_c^{(h\tau)}$ = escape prob. in zone $= \max(\tau, \text{hardcore}) \equiv h\tau$

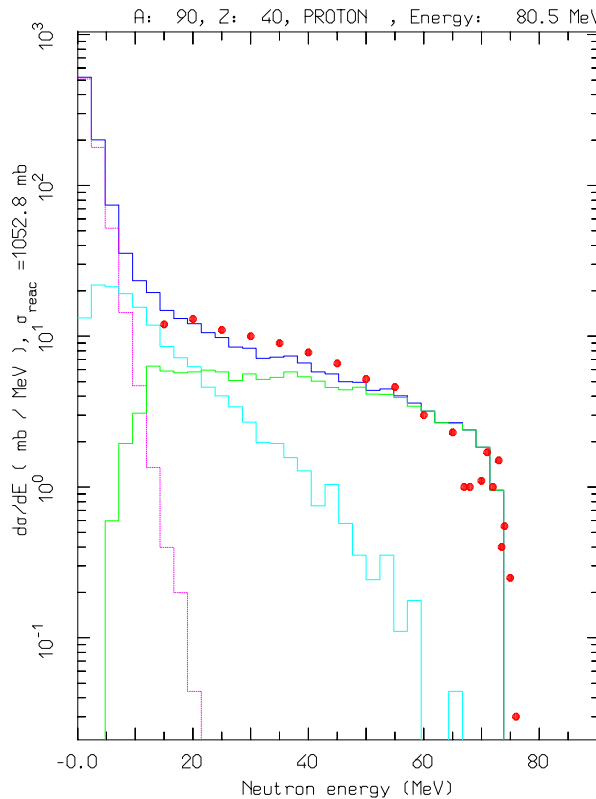
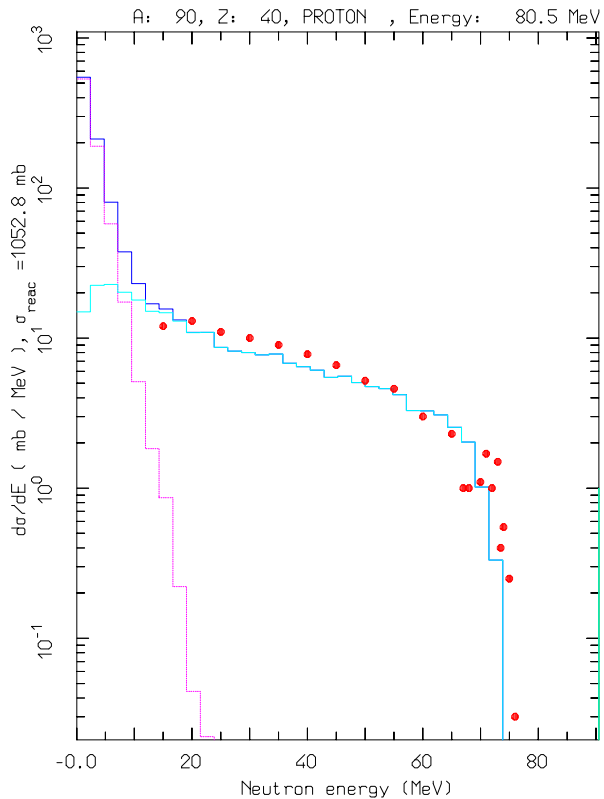
$P_c^{(co)}$ = escape/total prob. in zone $= (\text{correlation} - h\tau)$

(here reinteraction only on non-correlated nucleon specie)

$P_c^{(std)}$ = "standard" escape/total in remaining zone.

- Constrained exciton state densities configurations 1p-1h, 2p-1h, 1p-2h, 2p-2h, 3p-1h and 3p-2h
- Energy dependent form for g_x

Preequilibrium/(G)INC transition



Example of angle integrated $^{90}\text{Zr}(p, xn)$ at 80.5 MeV calculations with the full algorithm (right), and without the INC stage (left). The various lines show the total, INC, preeq. and evaporation contributions, the exp. data have been taken from M.Trabandt et al. PRC39 (1989) 452

Evaporation, fission and nuclear break-up

The evaporation probability for a particle of type j , mass m_j , spin $S_j \cdot \hbar$ and kinetic energy E and the total fission probability are given by
(i for initial nucleus, f for final, F at fission saddle point)

$$P_j = \frac{(2S_j + 1)m_j}{\pi^2 \hbar^3} \int_{V_j}^{U_i - Q_j - \Delta_f} \sigma_{\text{inv}} \frac{\rho_f(U_f)}{\rho_i(U_i)} E dE$$
$$P_F = \frac{1}{2\pi\hbar} \frac{1}{\rho_i(U_i)} \int_0^{(U_i - B_F)} \rho_F(U_i - B_F - E) dE$$

- ρ 's: nuclear level densities,
- U : excitation energy,
- V_j : (possible) Coulomb barrier for emitting a particle of type j
- Q_j : reaction Q for emitting a particle of type j ,
- σ_{inv} : cross section for the inverse process

For low mass residuals: **Fermi break-up:** statistical phase-space production of multiple (excited) fragments

Excitation energy **AFTER** evaporation $\rightarrow \gamma$ emission

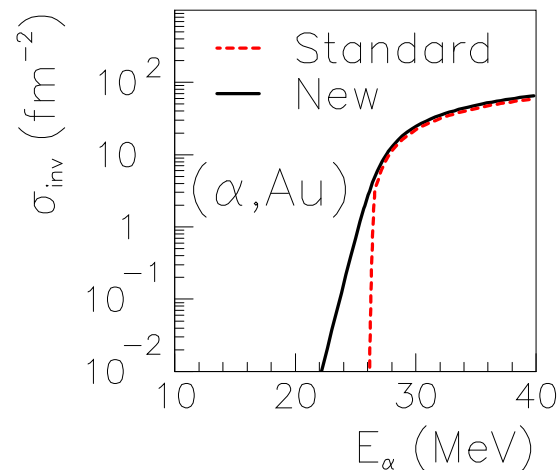
Evaporation

Latest Improvements to evaporation

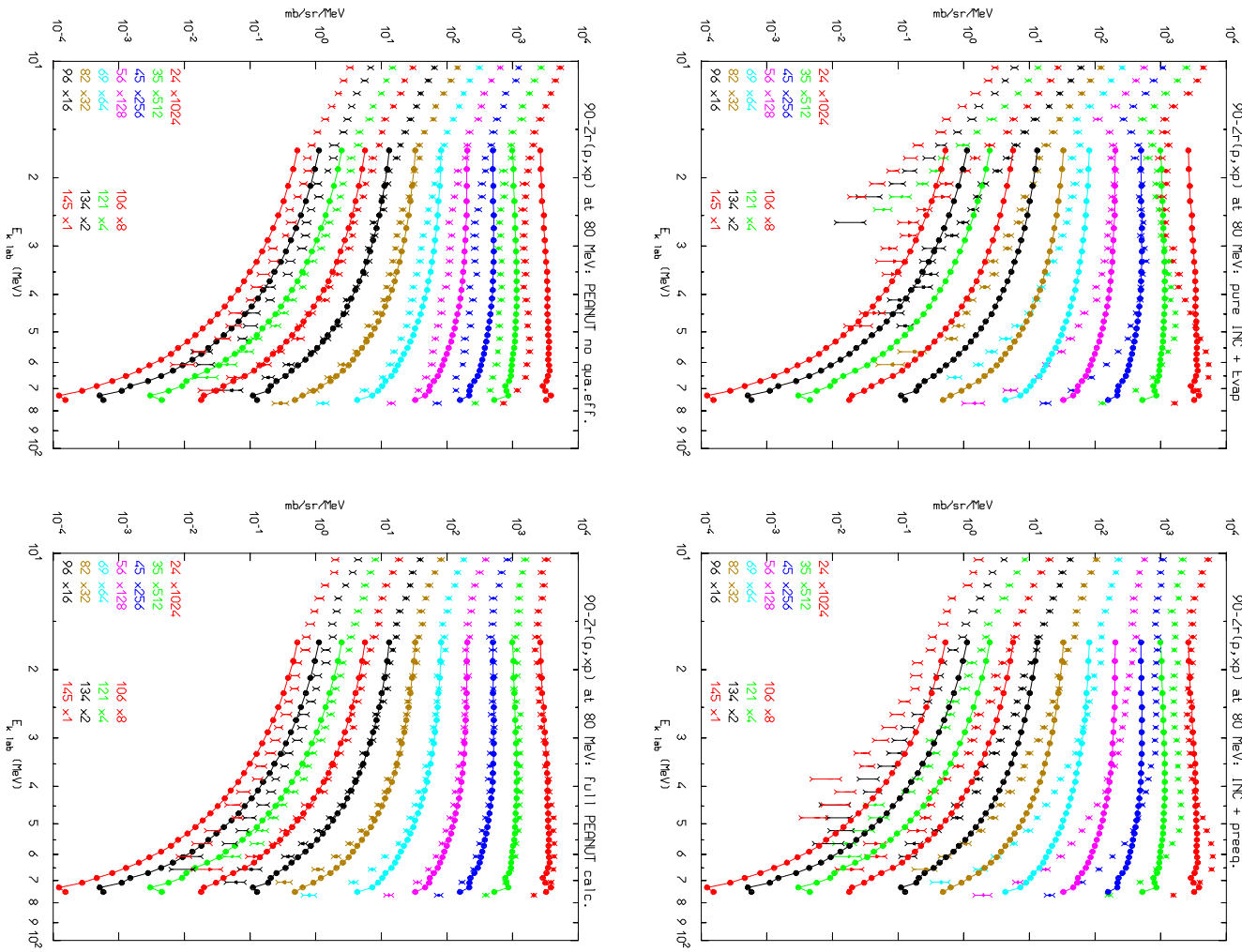
- Improved state density $\rho = \exp(2\sqrt{aU})/U^{5/4}$
- No Maxwellian approximation for energy sampling
- γ competition in progress

- Sub-barrier emission:

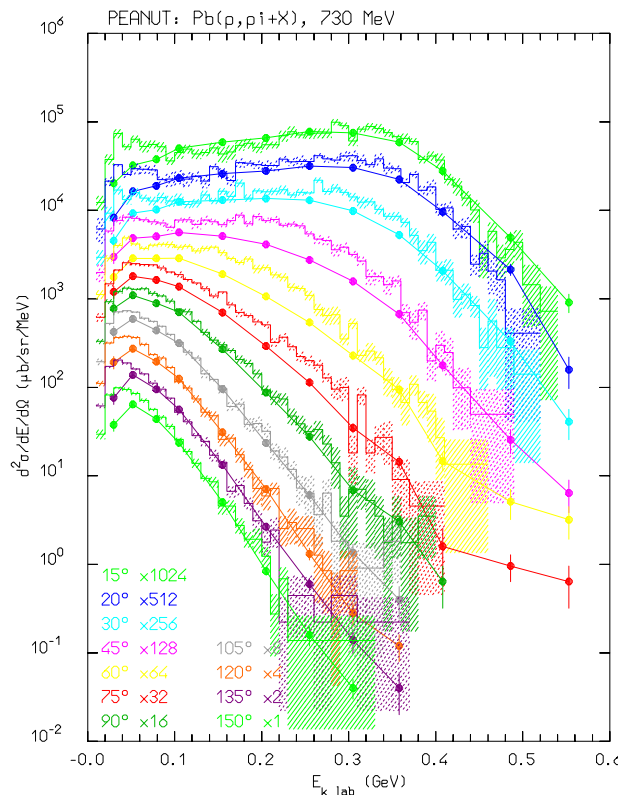
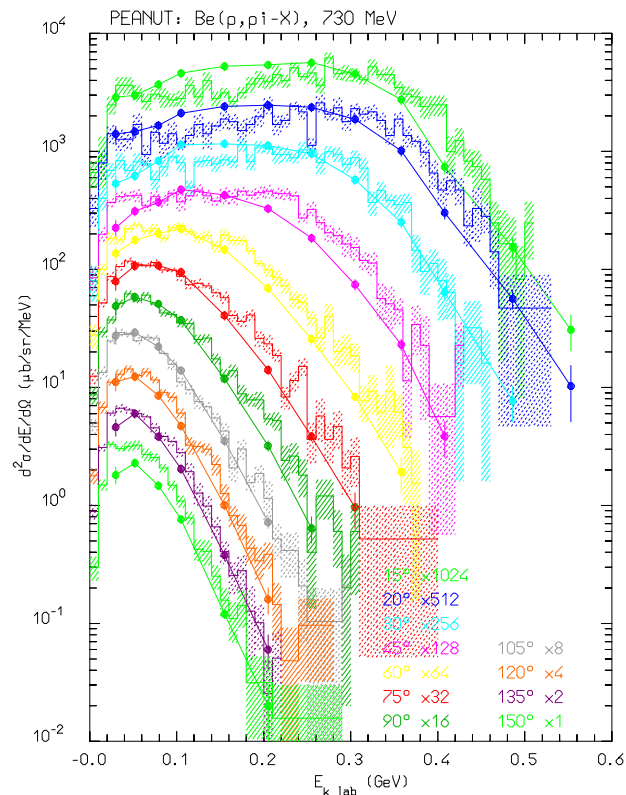
$$\sigma_{inv}^x = (R + \bar{\lambda})^2 \frac{\hbar\omega_x}{2E} \ln \left[1 + e^{\frac{2\pi(E - V_c)}{\hbar\omega_x}} \right]$$



Nucleon emission: thin target examples I

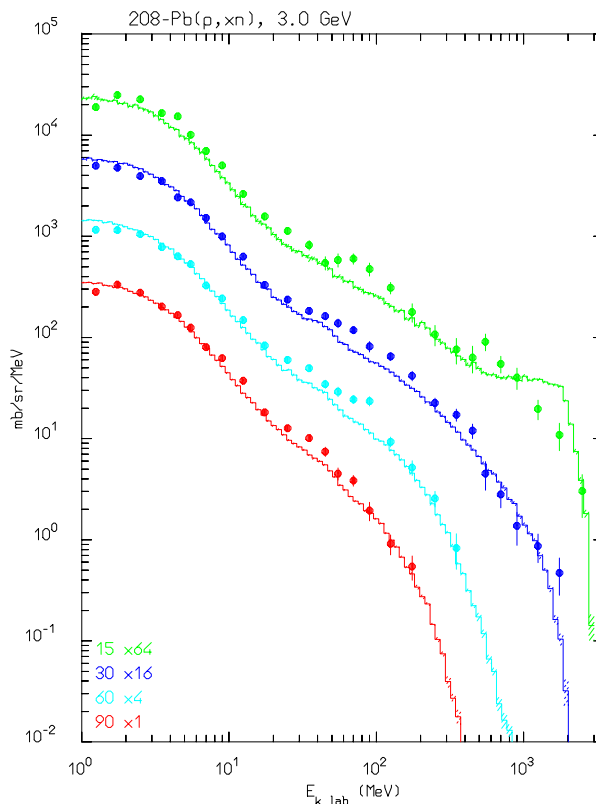
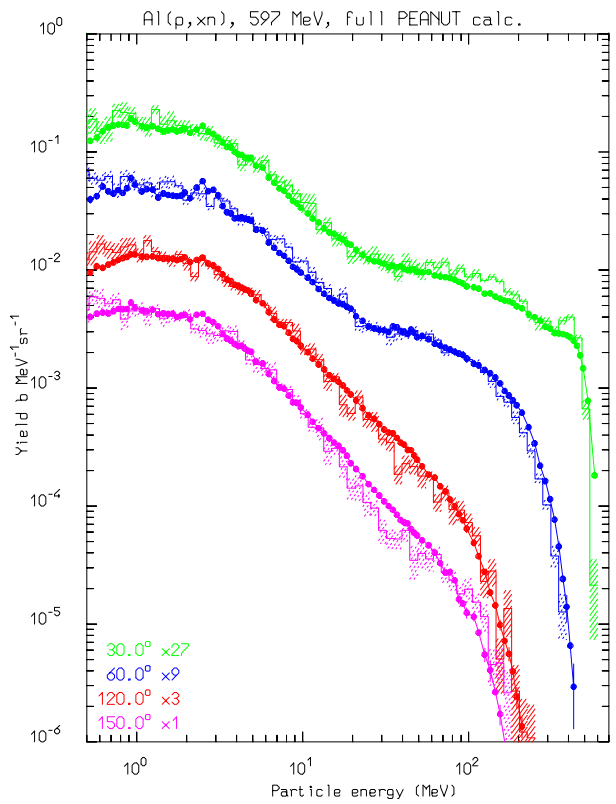


Nonelastic interactions at intermediate energies: examples II



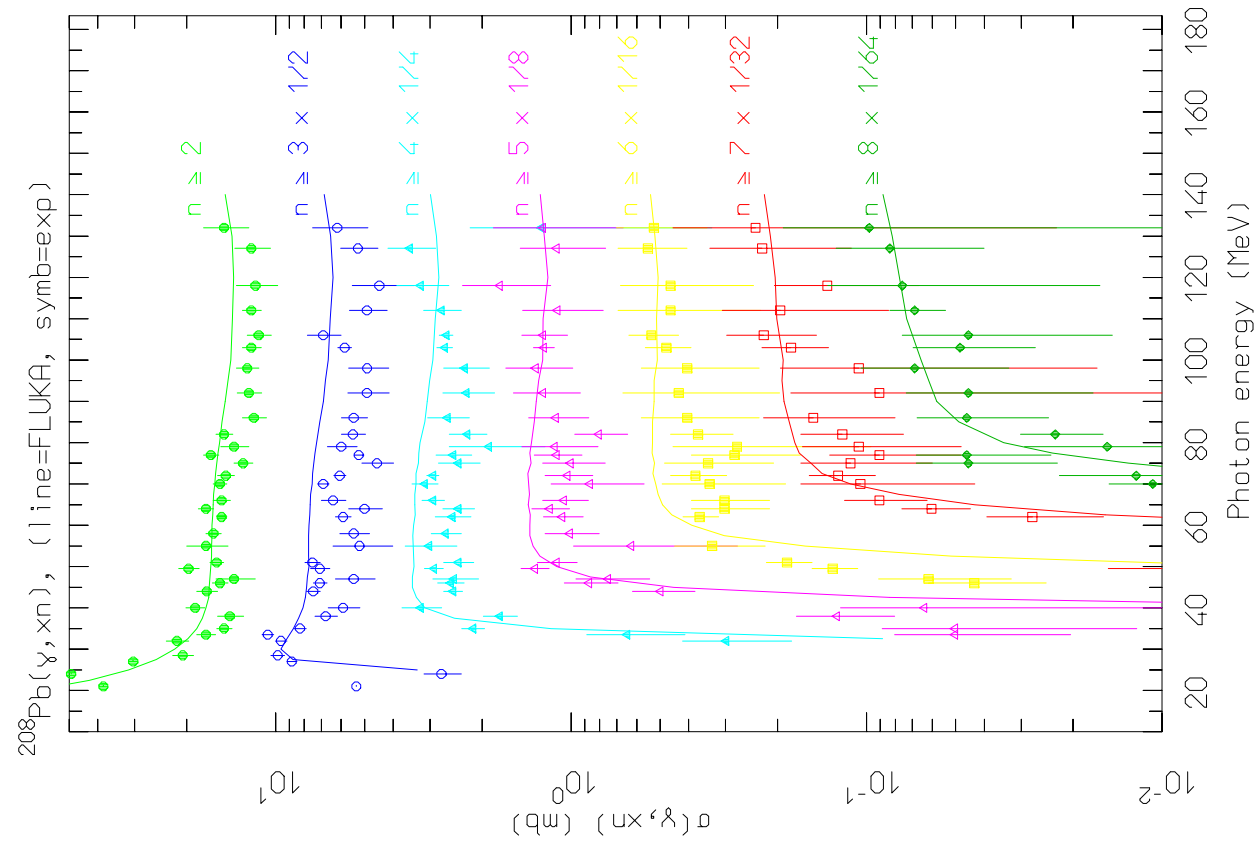
Double differential distributions of pions produced by 730 MeV protons. π^- 's from Be (left) and π^+ from Pb (right). Exp. data (symbols) have been taken from D.R.F. Cochran et al., PRD **6**, (1972)

Nucleon emission: thin target examples II



Computed (histograms) and experimental (symbols) double differential neutron distributions for Al(p,xn) (left) at 597 MeV and Pb(p,xn) at 3 GeV. The exp. data have been taken from W.B. Amian et al., Nucl. Sci. Eng. **115**, (1993) 1, and K. Ishibashi et al, Nucl. Sci. Technol. **32** (1995) 827.

Pb(γ ,xn) (exp. data NPA367, 237 (1981), NPA390, 221 (1982))



Nuclear density

Nuclear density

given by symmetrized Woods-Saxon for $A > 16$,

$$\begin{aligned}\rho(r) &= \rho_0 \frac{\sinh(R_0/a)}{\cosh(r/a) + \cosh(R_0/a)} \\ &\approx \frac{\bar{\rho}_0}{1 + \exp \frac{r-R_0}{a}}\end{aligned}\tag{1}$$

and by a harmonic oscillator shell model for light isotopes.

Simulated as 16 zones of constant density

Nuclear boundary at the radius (R_{nuc}) where $\rho = \rho_0/100$

Effect of nuclear and coulomb potentials also outside R_{nuc}

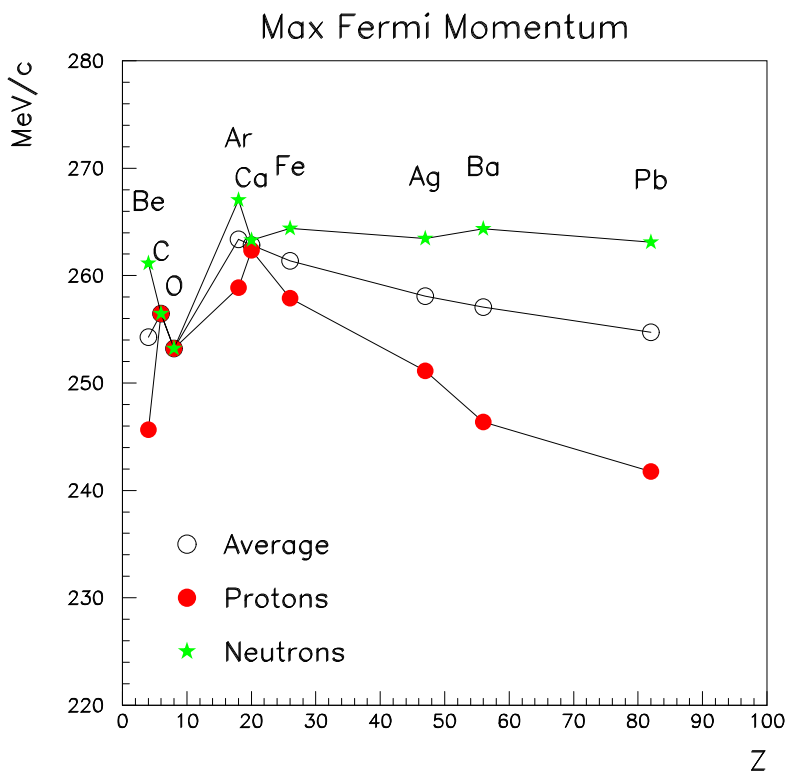
Proton and neutron densities are different (shell or droplet model)

Fermi momentum

Fermi momentum depends on the local density

$$k_F^{p,n}(r) = (3\pi^2 \rho^{p,n}(r))^{\frac{1}{3}} \quad (2)$$

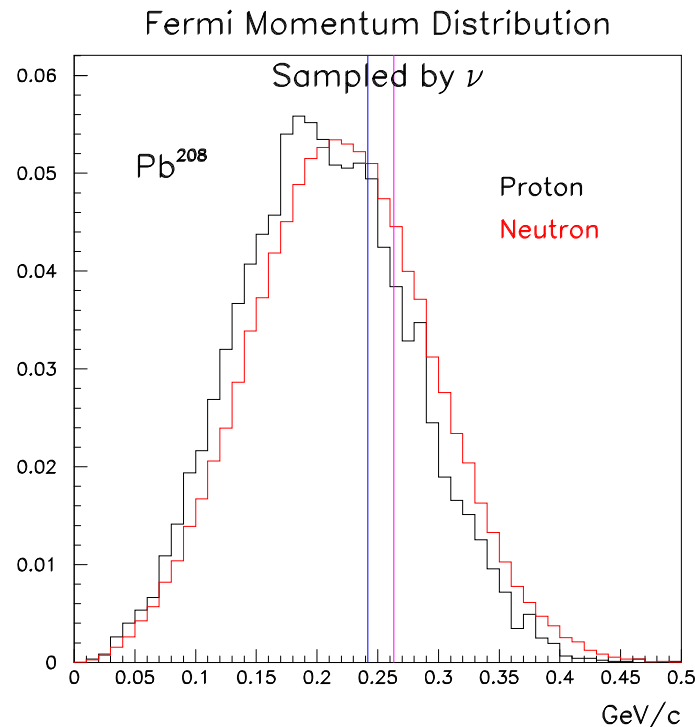
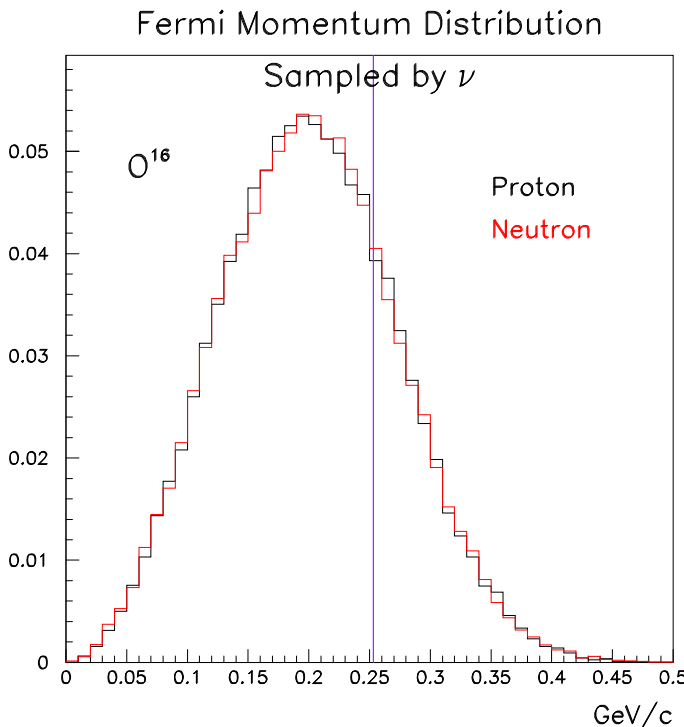
Momentum smearing according to uncertainty principle assuming a position uncertainty = $\sqrt{2} \text{ fm}$



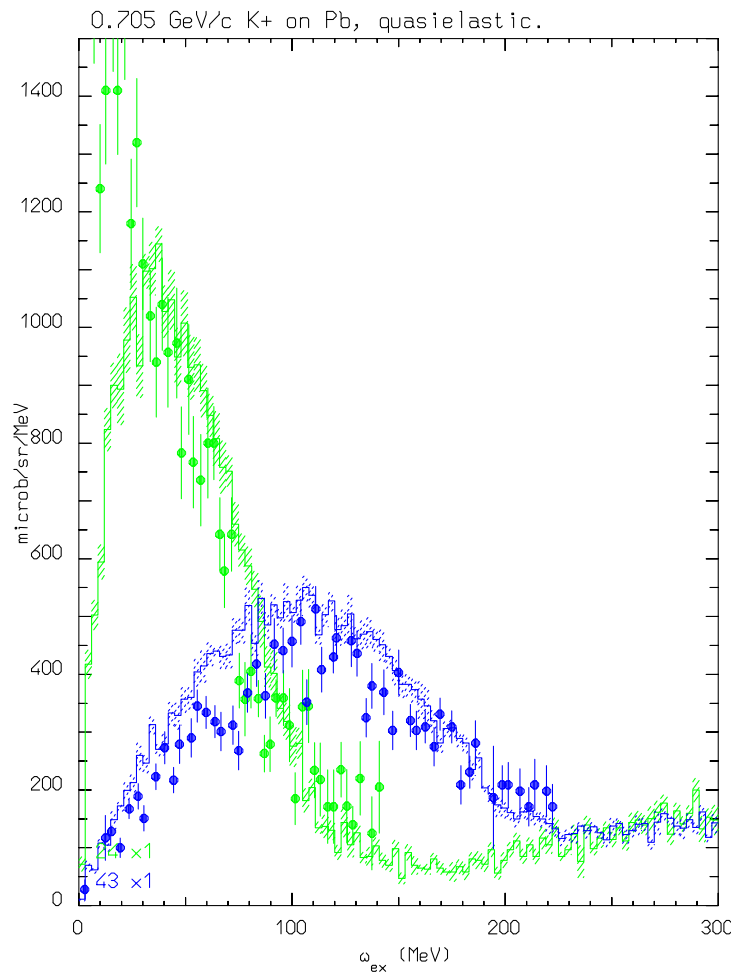
Fermi momentum

Fermi momentum distribution as sampled by ν_μ in ^{16}O and ^{208}Pb .

Proton and neutron distributions are shown together with un-smeared maximum from central density.



Test of Fermi motion: positive kaons



$K^+ \quad K^0$

No low mass $S=1$ baryons →
weak $K^+ N$ interaction
only elastic and ch. exch. up to
 ≈ 800 MeV/c

in PEANUT: $\frac{d\sigma}{d\Omega}$ from phase shift
analysis

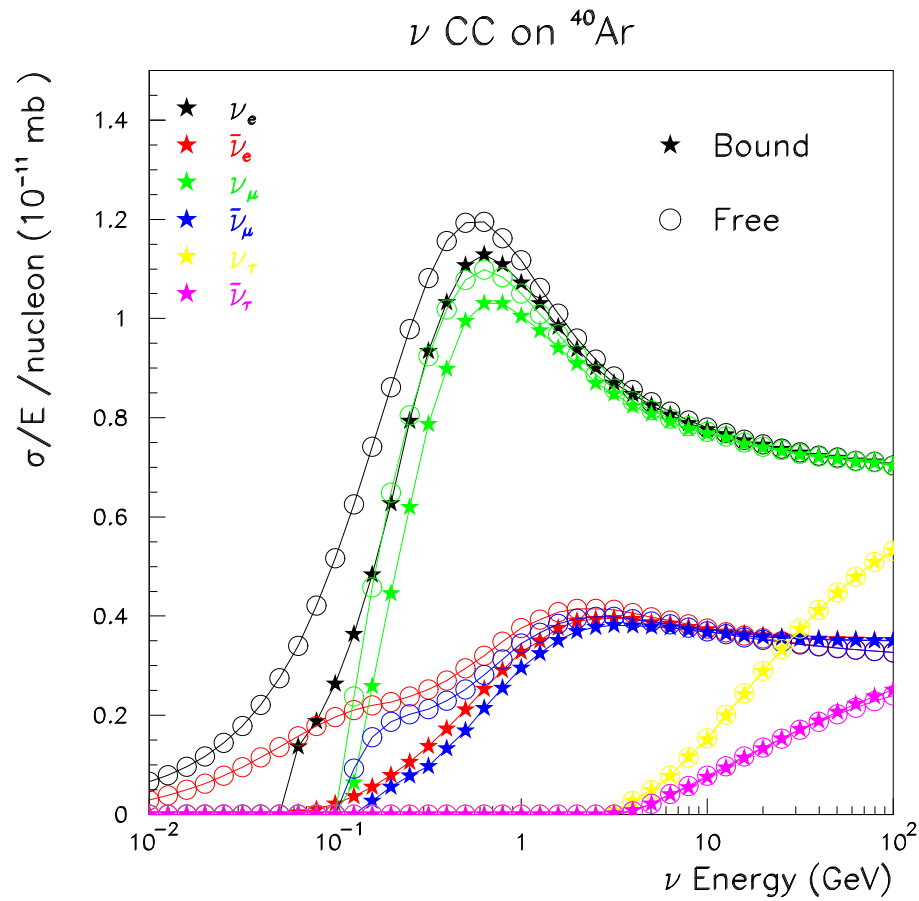
(K^+, K^{+}) on Pb vs residual excitation, 705 MeV/c, at 24° and 43° .

Histo: FLUKA, dots: data (Phys.
Rev. C51, 669 (1995))

On free nucleon: recoil energy :
43 MeV at 24° , 117 MeV at 43° .

Pauli

Pauli principle is taken into account
→ visible effect on σ .



Formation zone

Naively: “materialization” time. Qualitative estimate: in the frame where $p_{\parallel} = 0$

$$\bar{t} = \Delta t \approx \frac{\hbar}{E_T} = \frac{\hbar}{\sqrt{p_T^2 + M^2}}$$

particle proper time

$$\tau = \frac{M}{E_T} \bar{t} = \frac{\hbar M}{p_T^2 + M^2}$$

Going to lab system

$$t_{lab} = \frac{E_{lab}}{E_T} \bar{t} = \frac{E_{lab}}{M} \tau = \frac{\hbar E_{lab}}{p_T^2 + M^2}$$

Condition for possible reinteraction inside a nucleus:

$$v \cdot t_{lab} \leq R_A \approx r_0 A^{1/3}$$

Coherence length

Coherence length \equiv formation time for elastic or quasielastic interactions.

Given a two body interaction between with four-momentum transfer

$$q = p_{1i} - p_{1f}$$

the energy transfer seen in a frame where the particle 2 is at rest is given by

$$\Delta E_2 = \nu_2 = \frac{q \cdot p_{2i}}{m_2}$$

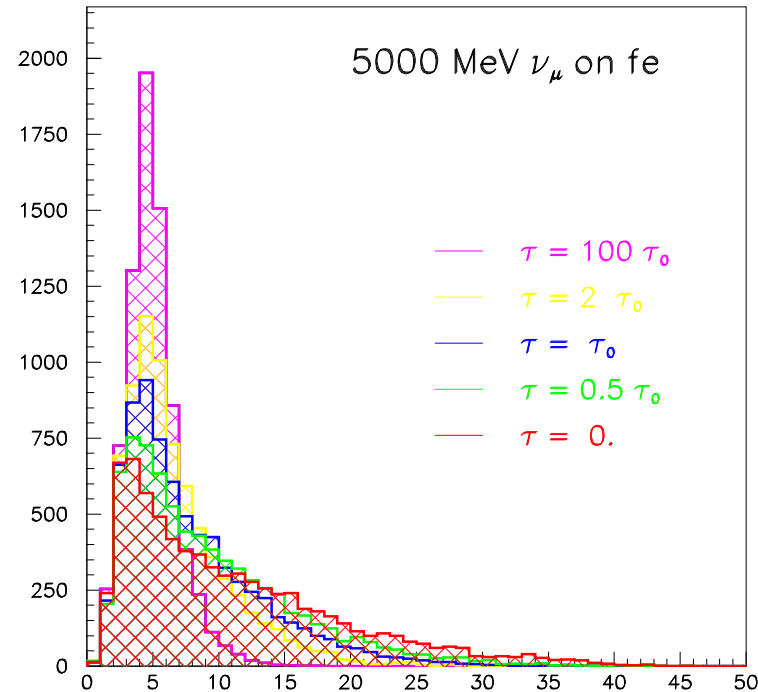
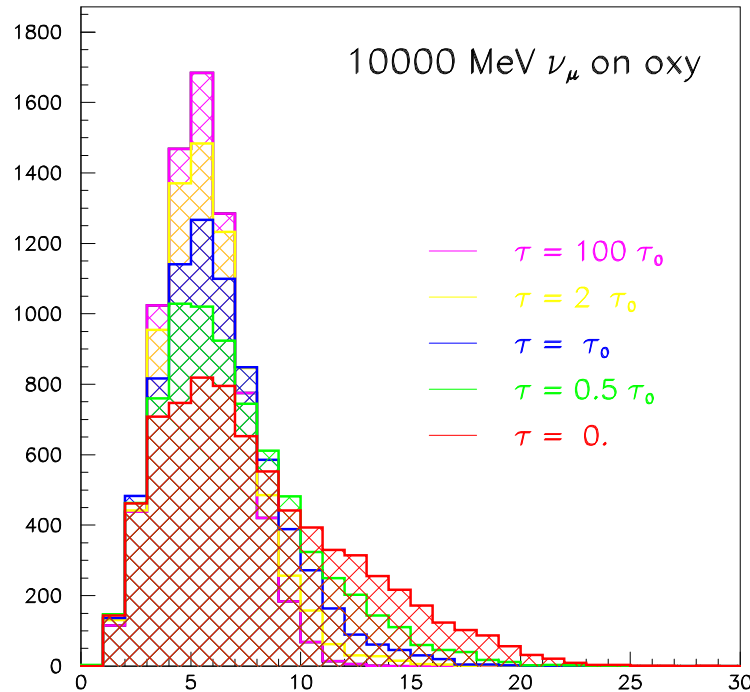
From the uncertainty principle this ΔE corresponds to a indetermination in proper time given by $\Delta\tau \cdot \Delta E_2 = \hbar$, that boosted to the lab frames gives a coherence length

$$\Delta x_{lab} = \frac{p_{2lab}}{m_2} \cdot \Delta\tau = \frac{p_{2lab}}{m_2} \frac{\hbar}{\nu_2}$$

And analogue for particle 1

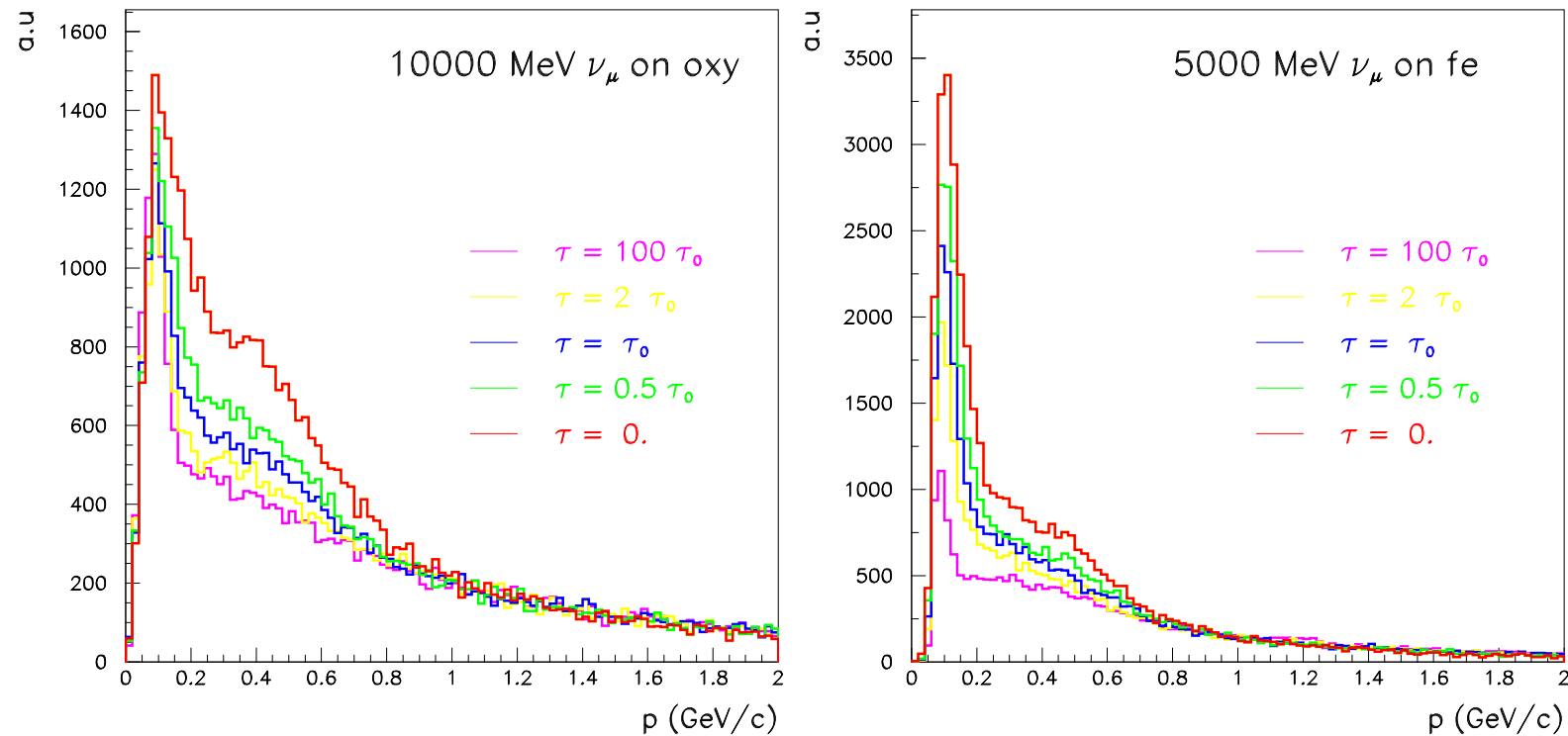
Formation zone+ coherence length effect

Effect of different formation time (τ) values on the total hadron multiplicity in ν_μ CC interactions.



Formation zone+ coherence length effect

Effect of different formation time (τ) values on the charged hadron spectra in ν_μ CC interactions.



Pions: optical potential

For pions, a complex nuclear potential can be defined out of the pion-nucleon scattering amplitude to be used in conjunction with the Klien-Gordon equation:

$$[(\omega - V_c)^2 - 2\omega U_{opt} - K^2] \Psi = m_\pi^2 \Psi$$

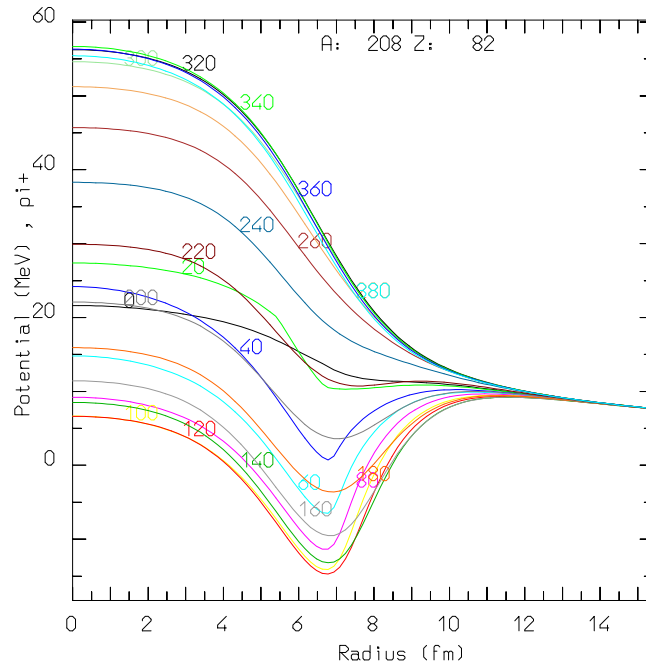
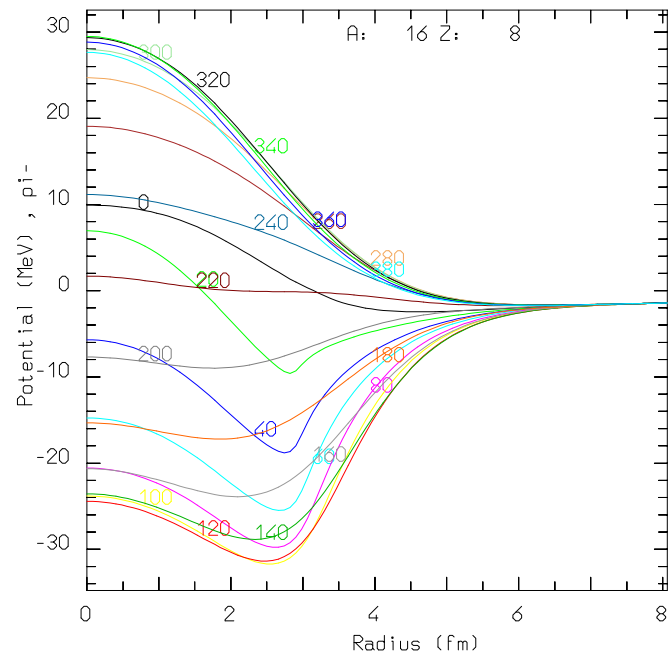
In coordinate space, this is written as (the upper/lower signs refer to π^+/π^-):

$$\begin{aligned} 2\omega U_{opt}(\omega, r) &= -\beta(\omega, r) + \frac{\omega}{2M} \nabla^2 \alpha(\omega, r) - \nabla \cdot \frac{\alpha}{1 + g\alpha(\omega, r)} \nabla \\ \beta &= 4\pi \left[\left(1 + \frac{\omega}{M}\right) \left(b_0(\omega) \mp b_1(\omega) \frac{N-Z}{A}\right) \rho(r) + \left(1 + \frac{\omega}{2M}\right) B_0(\omega) \rho^2(r) \right] \\ \alpha &= 4\pi \left[\frac{1}{1 + \frac{\omega}{M}} \left(c_0(\omega) \mp c_1(\omega) \frac{N-Z}{A}\right) \rho(r) + \frac{1}{1 + \frac{\omega}{2M}} C_0(\omega) \rho^2(r) \right] \end{aligned}$$

Using standard methods to get rid of the non-locality, in momentum space

$$\begin{aligned} 2\omega U_{opt}(\omega, K) &= -\beta - K^2 \frac{\alpha}{1 + g\alpha} + \frac{\omega}{2M} \nabla^2 \alpha \\ K^2 &= k_0^2 + V_c^2 - 2\omega V_c^2 - 2\omega U_{opt}(\omega, K) = \frac{k_0^2 + V_c^2 - 2\omega V_c^2 + \beta - \frac{\omega}{2M} \nabla^2 \alpha}{1 - \bar{\alpha}} \\ \bar{\alpha} &= \frac{\alpha}{1 + g\alpha} \end{aligned}$$

Pion optical potential examples



The real part of the pion optical potential for π^- on ^{16}O (left) and π^+ on ^{208}Pb (right) as a function of radius for various pion energies (MeV)

Pions: nuclear medium effects

Pion-nucleon interactions: non-resonant + p -wave resonant Δ 's.

decay	Δ in nuclear medium	reinteraction
elastic scattering or charge exchange		pion absorption
$\rightarrow \Delta$ width different from the free one		

Assuming a Breit-Wigner for the free resonant cross section with width Γ_F

$$\sigma_{res}^{Free} = \frac{8\pi}{p_{cm}^2} \frac{M_\Delta^2 \Gamma_F(p_{cm})^2}{(s - M_\Delta^2)^2 + M_\Delta^2 \Gamma_F(p_{cm})^2}$$

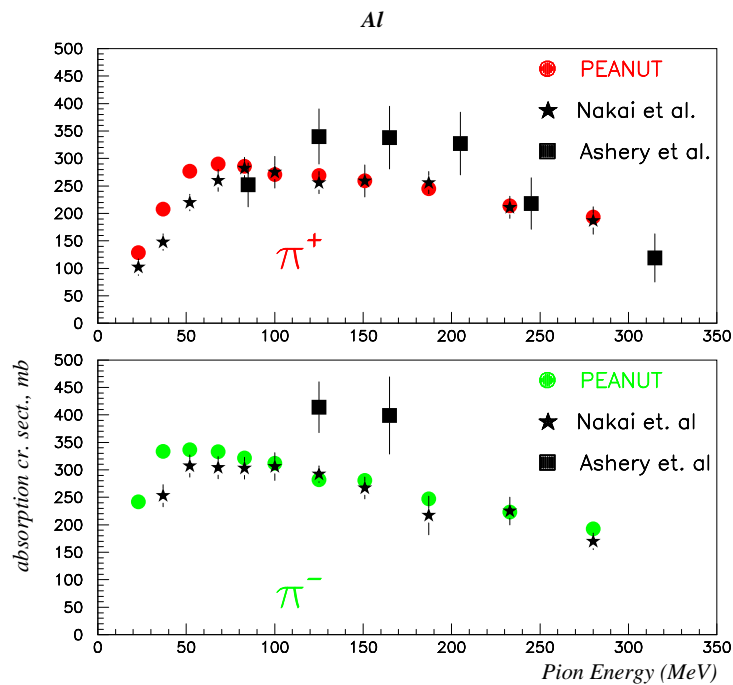
Add “in medium” width (Oset et.al ,NPA 468, 631)

$$\frac{1}{2}\Gamma_T = \frac{1}{2}\Gamma_F - \text{Im}\Sigma_\Delta, \quad \Sigma_\Delta = \Sigma_{qe} + \Sigma_2 + \Sigma_3$$

(Σ_{qe} , Σ_2 , Σ_3 = widths for quasielastic scattering, two and three body absorption)

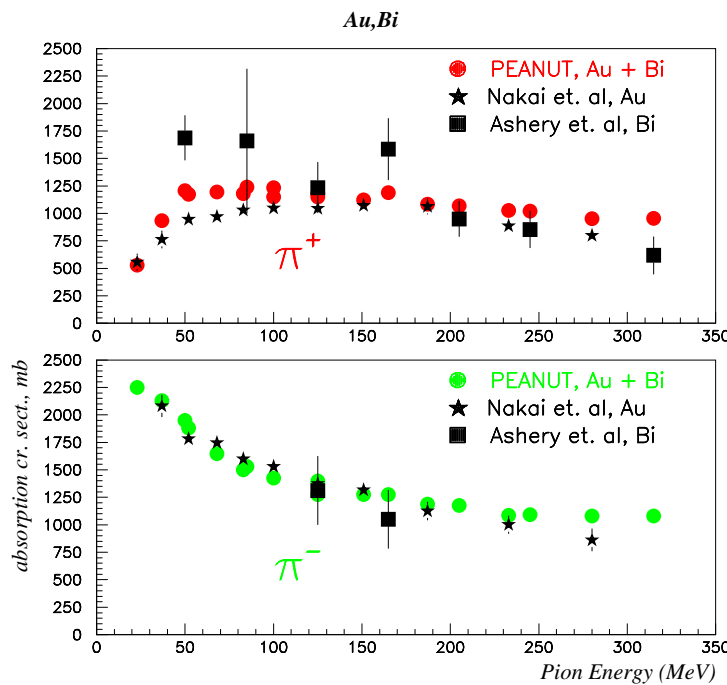
Add two-body s -wave absorption cross section from optical model

Pion absorption cross sections: examples



Computed and exp. pion absorption cross section on Aluminum as a function of energy

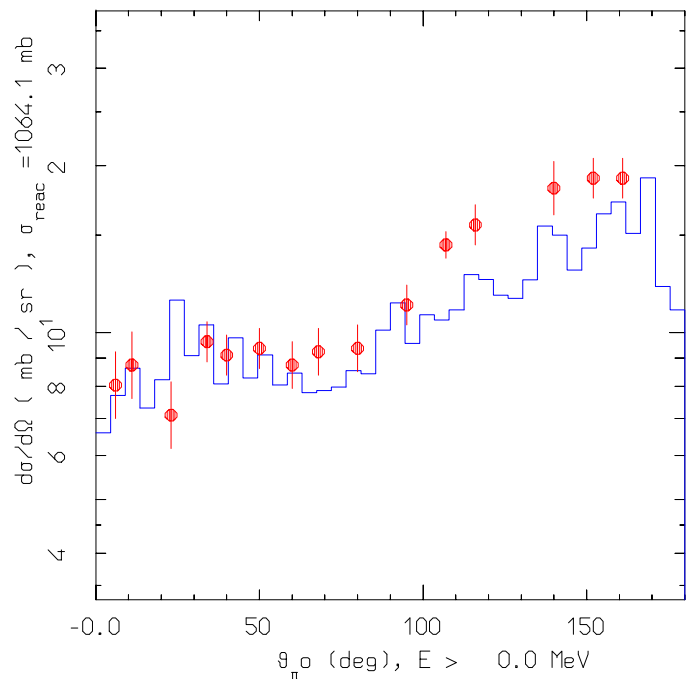
(Exp. data: D. Ashery et al., **PRC23**, (1981) 2173 and K. Nakai et. al., **PRL44**, (1979) 1446)



Computed and exp. pion absorption cross section on Gold or Bismuth as a function of energy

Pion-nucleus interactions: examples

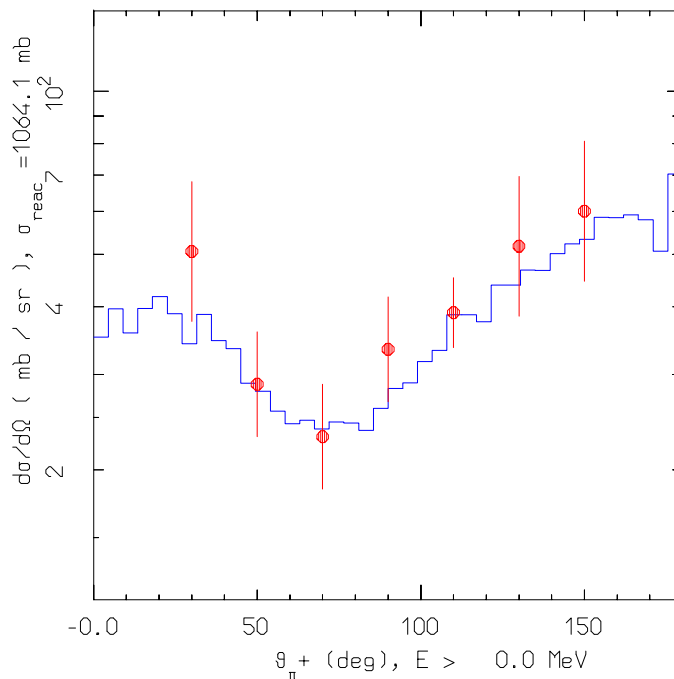
A: 58, Z: 28, PION+, Energy: 160.0 MeV



Computed and exp. pion charge exchange angular distribution for $^{58}\text{Ni}(\pi^+, \pi^0)$ at 160 MeV

(Exp. data: W.J. Burger et al., PRC41, (1990) 2215 and R.D. McKeown et al., PRC24, (1981) 211)

A: 58, Z: 28, PION+, Energy: 160.0 MeV



Computed and exp. pion inelastic angular distribution for $^{58}\text{Ni}(\pi^+, \pi^+')$ at 160 MeV

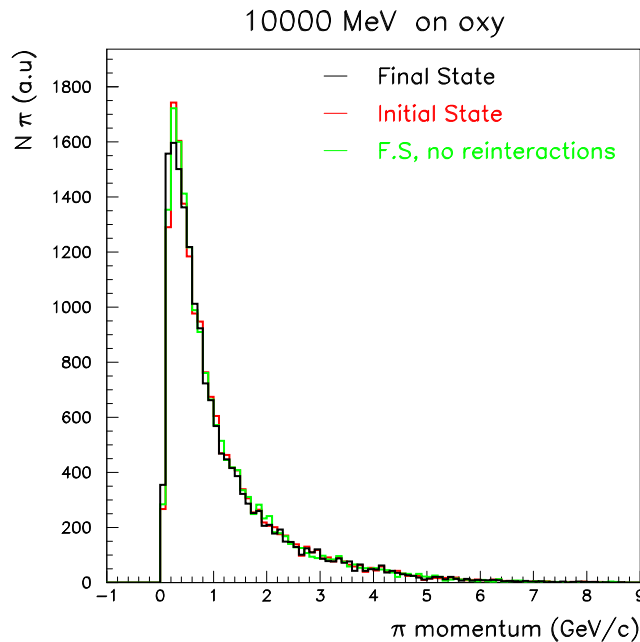
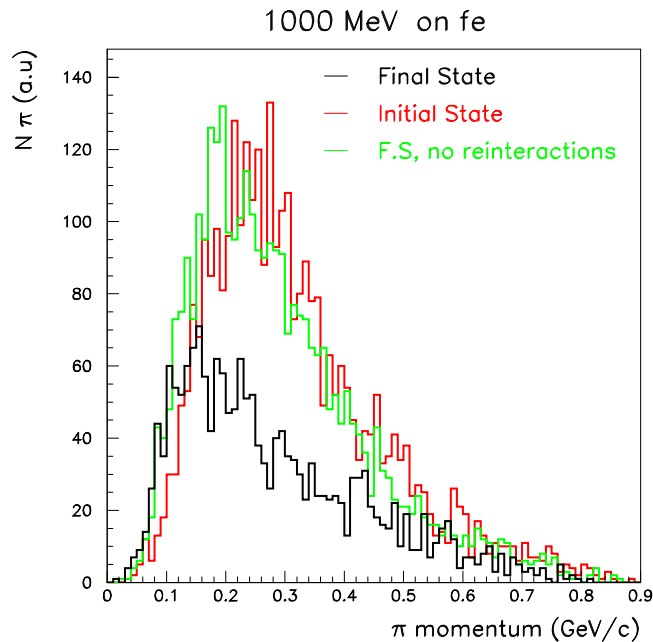
Pions in ν interactions

Charged pion spectra after ν_μ interaction.

Initial State == particles still inside the nucleus

Final State == particles outside the nucleus

No reinteractions == only the effect of potentials



Only 55% escape at 1 GeV on Fe, 75% on Oxygen

observables

Nuclear effects with rough particle level reconstruction:

Experimentally, some reaction products can hardly be reconstructed as independent tracks:

even with ICARUS technology:

Protons below ≈ 50 MeV kinetic energy (travels 2.3 cm in LAr)

Charged pions below ≈ 15 MeV kinetic

Residual nuclei and heavy fragments

Low energy neutrons

Low energy (nuclear deexcitation) photons

with Water Cerenkov: particle momentum thresholds

Electron 0.6 MeV/c

Muon 120 MeV/c

Pion 159 MeV/c

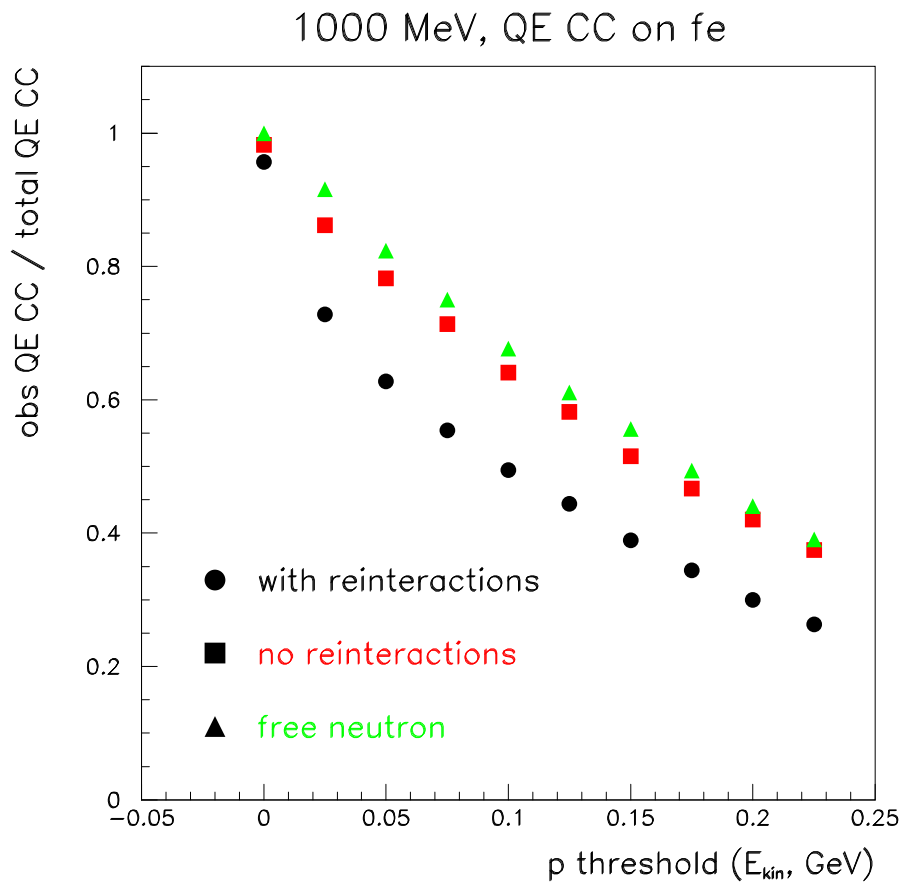
Kaon 568 MeV/c

Proton 1070 MeV/c

Channel id/ QE vs thr

Let's define
ICARUS QE CC =
1 charged lepton
no pions above cut
 ≥ 1 proton above cut

acceptance =
$$\frac{QE\ CC}{\text{original QE CC}}$$

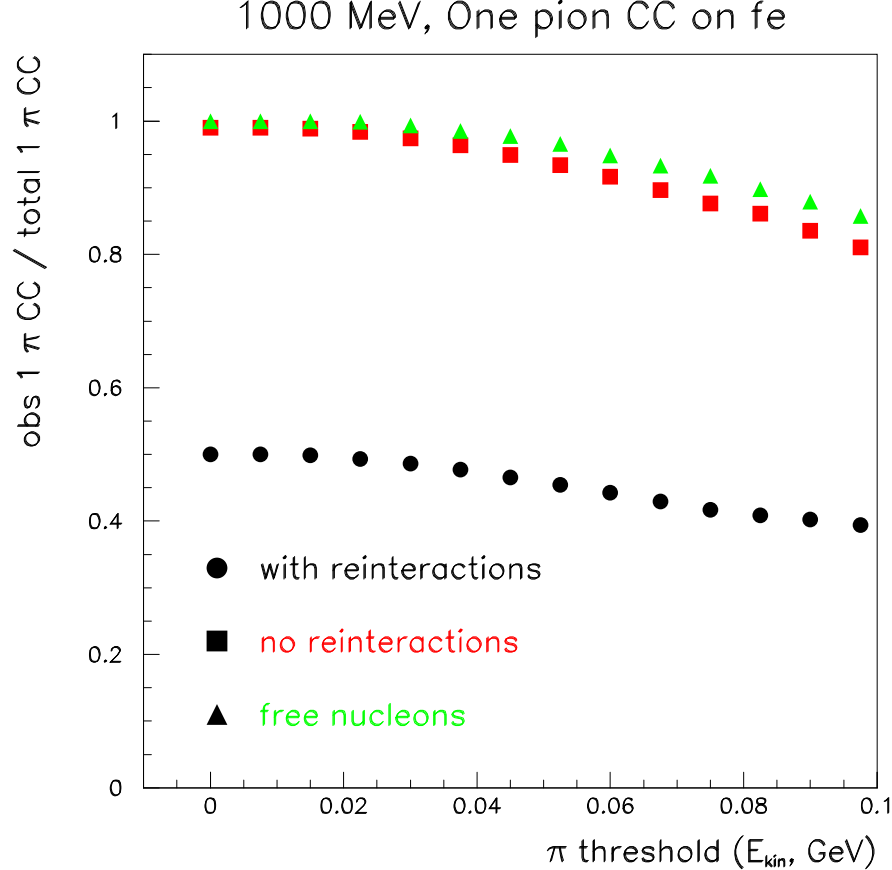


Protons are lost due to reinteractions and binding

Channel id/ One Pion vs threshold

Let's define
ICARUS One π CC =
1 charged lepton
1 π above cut

acceptance =
$$\frac{\text{One } \pi \text{ CC}}{\text{original } 1 \pi \text{CC}}$$

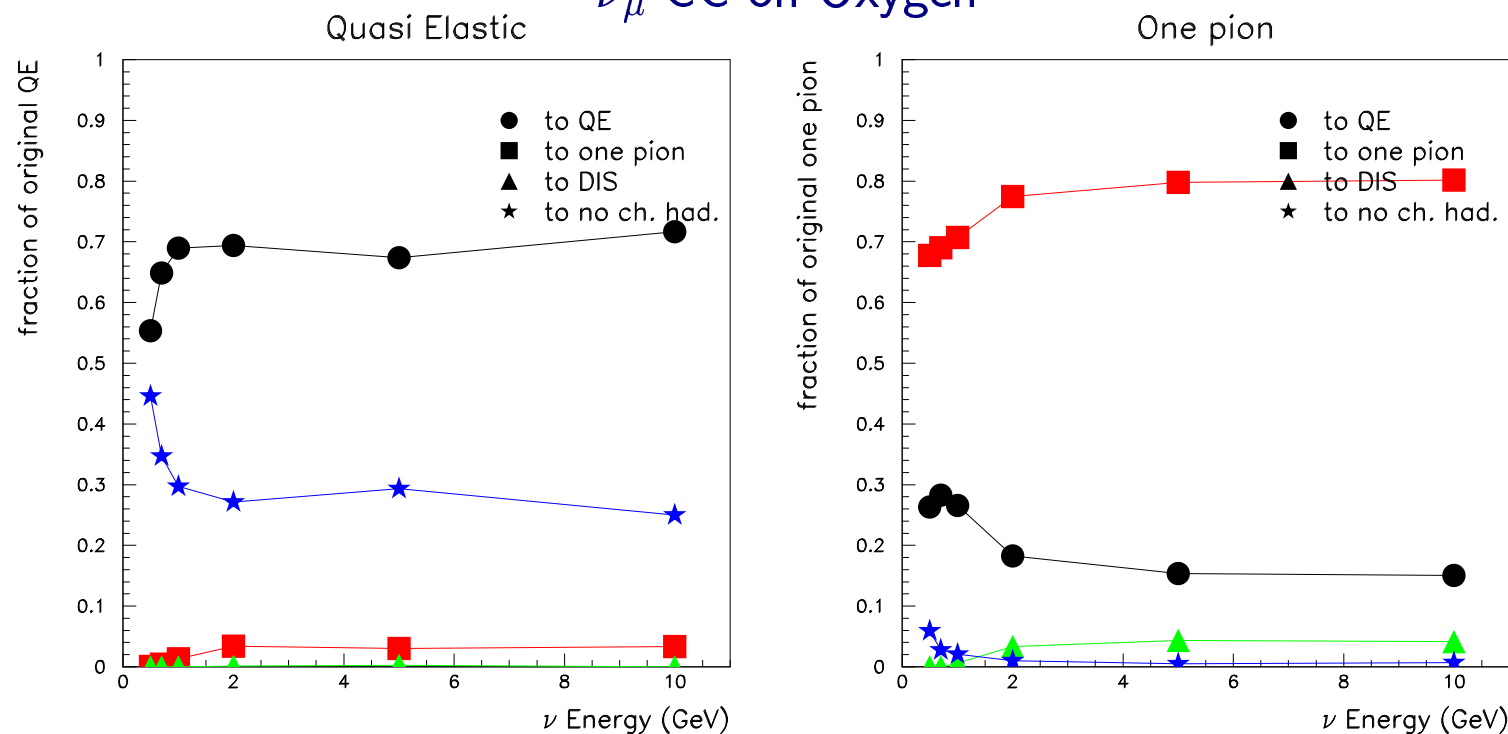


Pion reinteractions make the difference

Channel id/ QE and one pion

ICARUS cuts, 50 MeV kinetic for protons, 15 MeV for π

ν_μ CC on Oxygen

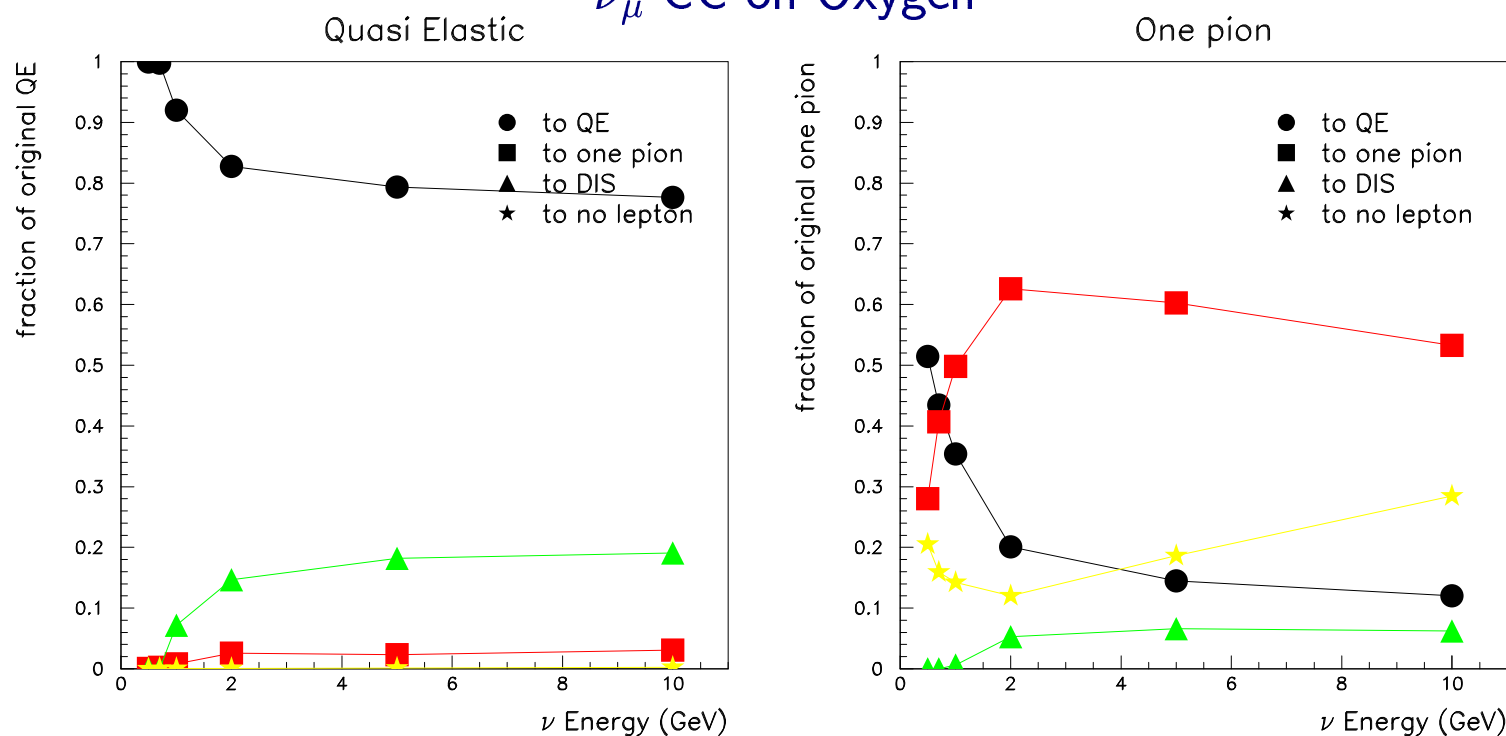


reaction channels mix together

Channel id/ QE and one pion

Water Cerencov cuts, QE = single ring , one pion = 1 lepton + 1 pion

ν_μ CC on Oxygen



reaction channels mix together, even more

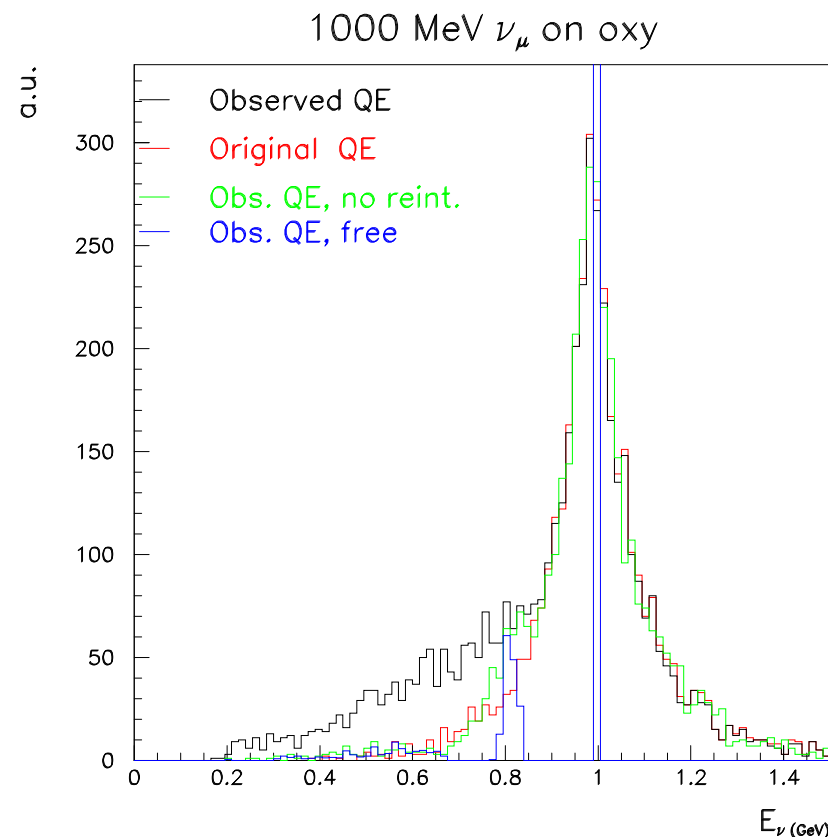
QE E_ν reconstruction

Water Cerencov cuts

ν_μ CC on Oxy

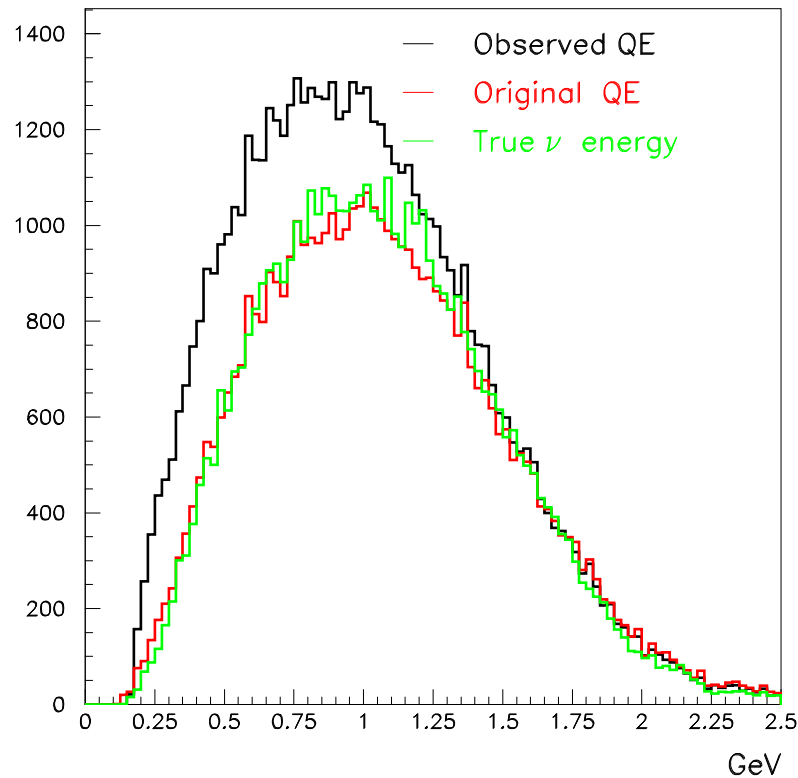
Reconstructed ν energy
in QE (== single ring)

$$E_\nu = \frac{M \cdot E_l - 0.5 \cdot m_l^2}{M - E_l + p_l \cdot \cos(\theta)}$$



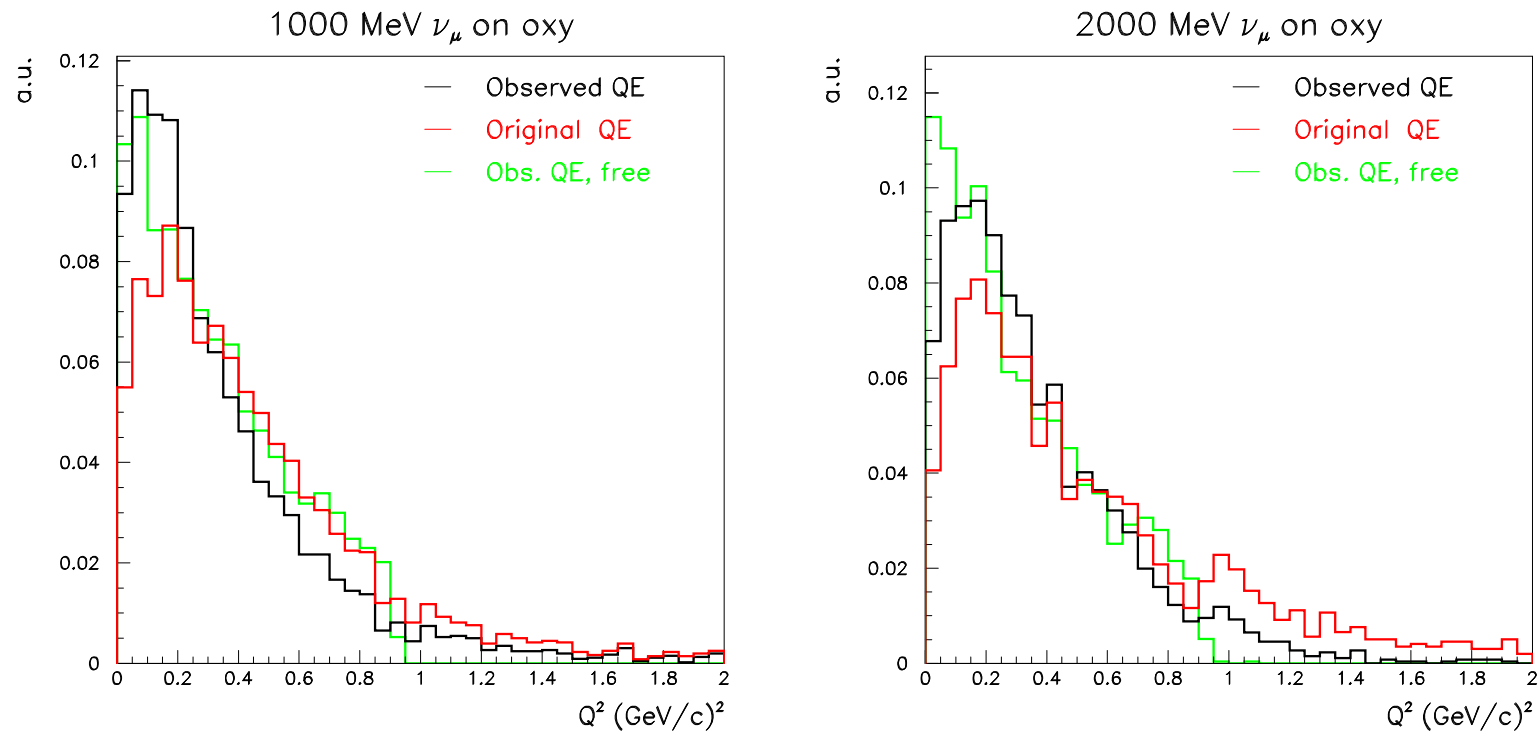
QE E_ν reconstruction

Water Cerencov cuts
MiniBoone spectrum
 ν_μ CC on Oxy
Reconstructed ν energy
in QE (== single ring)



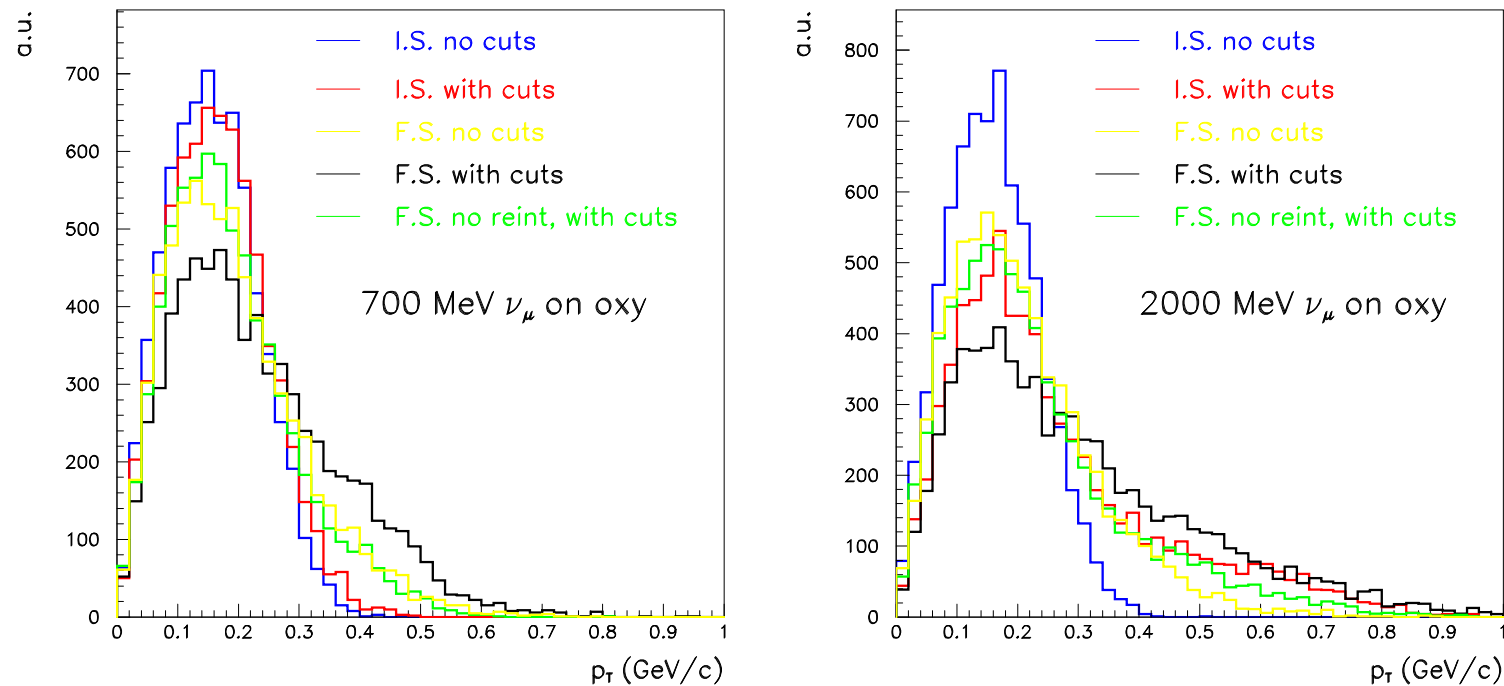
QE Q^2 reconstruction

ν_μ CC on Oxy, Reconstructed Q^2 in QE (== single ring).
 Water Cerencov cuts. Normalized to area.



Transverse momentum

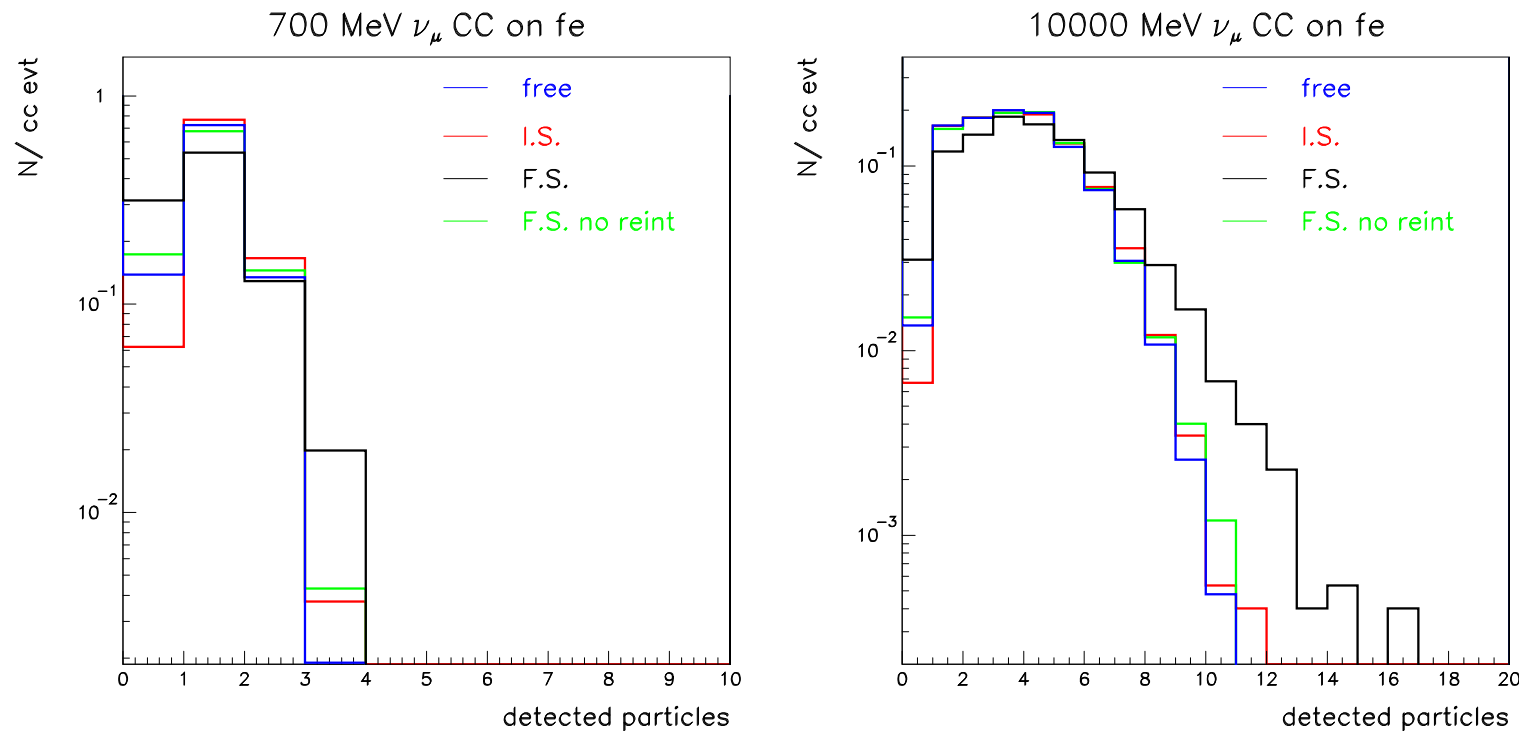
Standard ICARUS cuts: 50 MeV kinetic on protons, 15 MeV on pions



At low E_ν is dominated by Fermi, but reinteractions are important

Observed multiplicity

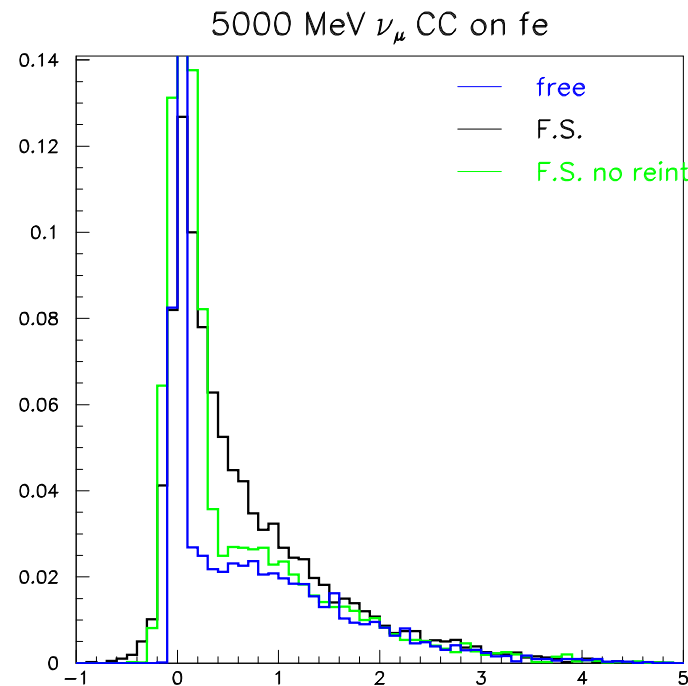
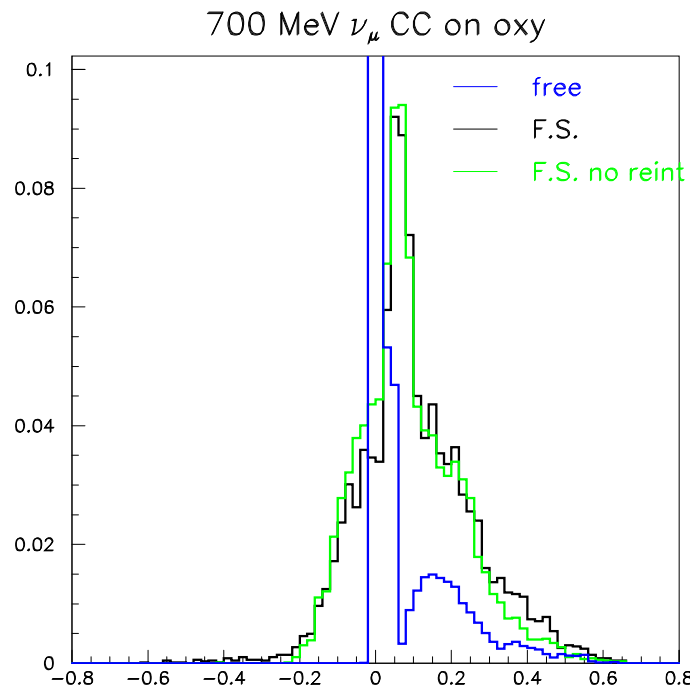
ICARUS cuts; observed hadron multiplicity in ν_μ CC interactions.



High multiplicity tails come from reinteractions

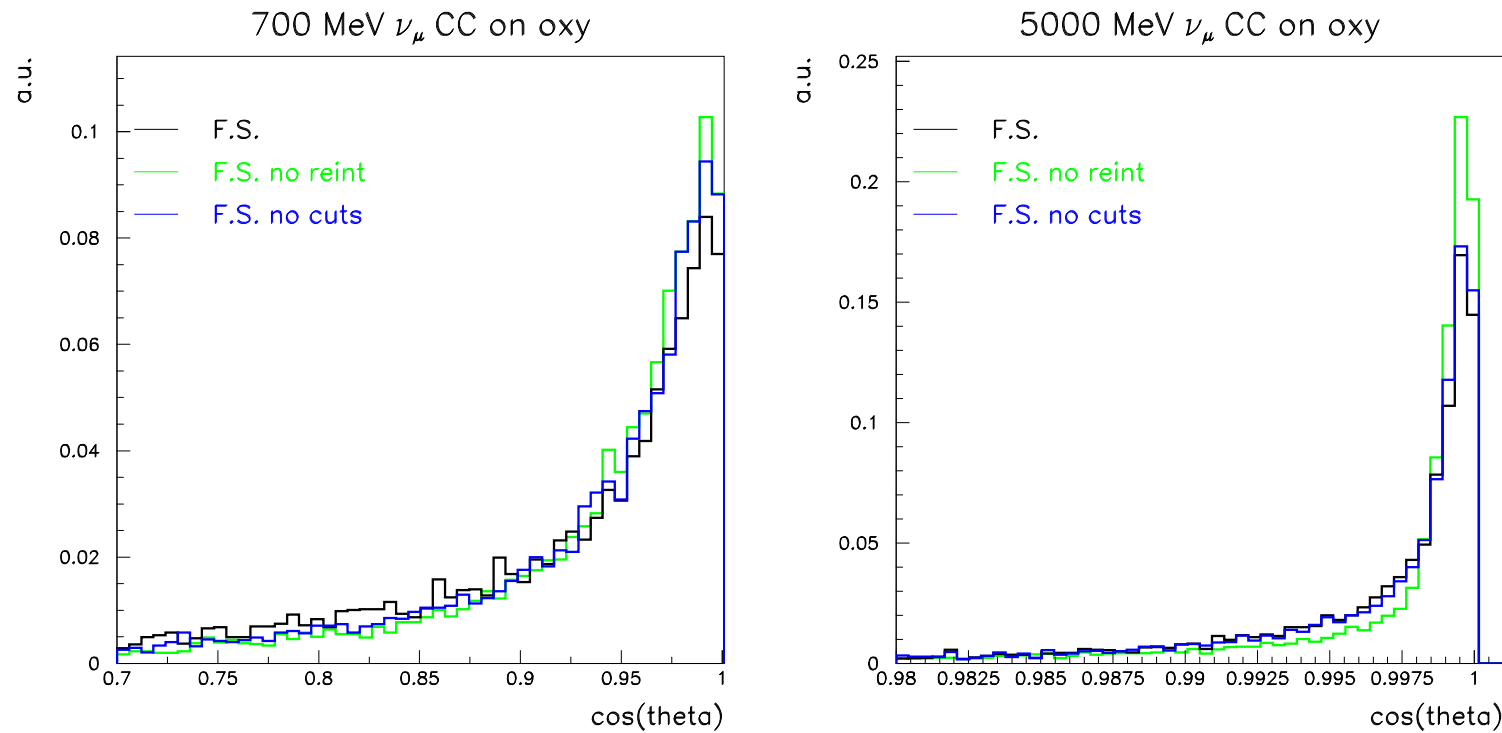
total missing momentum

Observed missing momentum in ν_μ CC interactions, ICARUS cuts



Reconstructed direction

Angle between reconstructed and real ν direction, in ν_μ CC interactions,
ICARUS cuts



Conclusions

The FLUKA nuclear interaction model has proven capabilities in hadron and photon induced reactions

Nuclear effects, both on initial state and on final state, affect all kinematic quantities

NUX-FLUKA has successfully simulated NOMAD data

It is already a reliable instrument for ν -nucleus interactions

Improvements , additions.. planned

Detector specific effects are also important

The best possible detector should be used to minimize the impact of nuclear effects, and improve their understanding.